Cardiac MyD88 Mediates Inflammatory Injury and Adverse Remodeling in Diabetes

Wu Luo
Wenzhou Medical University
Gaojun Wu
Wenzhou Medical University First Affiliated Hospital: The First Affiliated Hospital of Wenzhou Medical University
Xiaojun Chen
Wenzhou Medical University
Qiuyan Zhang
Wenzhou Medical University
Chunpeng Zou
Wenzhou Medical College Second Affiliated Hospital: Wenzhou Medical University Second Affiliated Hospital
Jun Liu
Wenzhou Medical University First Affiliated Hospital: The First Affiliated Hospital of Wenzhou Medical University
Nipon Chattipakorn
Chiang Mai University
Yi Wang
Wenzhou Medical University
Guang Liang (wzmcliangguang@163.com)
Wenzhou Medical University

Original investigation

Keywords: MyD88, diabetic cardiomyopathy, inflammation, fibrosis, cardiomyocytes

Posted Date: July 28th, 2021

DOI: https://doi.org/10.21203/rs.3.rs-744949/v1

Abstract

Background: Hyperglycemia-associated inflammation contributes to adverse remodeling and fibrosis in diabetic heart. MyD88 is an adapter protein of many Toll-like receptors (TLRs) and is recruited to TLRs to initiate inflammatory signalling pathway in endotoxin-activated innate immunity. However, the role of MyD88 in diabetic cardiomyopathy is unknown.

Methods: For genetic deficiency, cardiomyocyte-specific MyD88 knockout and littermate control mice were induced type 1 diabetes (T1D) by intraperitoneal injection of 50 mg/kg/day streptozotocin for five days consecutive and then fed for 4 moths. For pharmacological inhibition, MyD88 inhibitor LM8 were administered daily for 8 weeks by oral gavage in T1D and T2D (db/db) mice. The effect of genetic and pharmacological inhibition MyD88 to myocardial injure which were induced by 33 mM glucose in vivo.

Results: In this study, we first found that MyD88 expression was increased in cardiomyocytes of diabetic mouse hearts. Cardiomyocyte-specific MyD88 knockout protected mice against hyperglycemia-induced cardiac inflammation, injury, hypertrophy, and fibrosis in T1D model. In cultured cardiomyocytes, MyD88 inhibition either by siRNA or by small-molecular inhibitor LM8 markedly blocked TLR4-MyD88 complex formation, reduced pro-inflammatory MAPKs/NF-κB cascade activation and decreased pro-inflammatory cytokine expression under high glucose condition. Moreover, pharmacologic inhibition of MyD88 by LM8 showed significantly anti-inflammatory, anti-hypertrophic and anti-fibrotic effects in the hearts of both T1D and T2D mice. These beneficial effects of MyD88 inhibition were correlated to the reduced activation of TLR4-MyD88-MAPKs/NF-κB signaling pathways in the hearts.

Conclusion: Taken together, MyD88 in cardiomyocytes mediates diabetes-induced cardiac inflammatory injuries and genetic or pharmacologic inhibition of MyD88 shows significantly cardioprotective effects, indicating MyD88 as a potential therapeutic target for diabetic cardiomyopathy.

Introduction

Diabetic cardiomyopathy is characterized by chronic inflammation, cardiac fibrosis, adverse remodeling, diastolic dysfunction, systolic dysfunction, and eventually by clinical heart failure.[1] Heart failure rate in diabetic patients ranges between 19–26% and increases with the glycemic level.[2] The characteristic maladaptive pro-inflammatory or impaired innate immune response in type 1 and type 2 diabetes (T1D and T2D) is one of the most important instigators of diabetic cardiomyopathy.[2, 3] Diabetes-associated maladaptive inflammatory response leads to an increased expression and activation of proinflammatory cytokines, such as tumor necrosis factor α (TNF-α), interleukins 6 (IL-6), and interleukins 1β (IL-1β), which cause cardiac inflammation, adverse remodeling and fibrosis, and diastolic dysfunction.[4]

Myeloid differentiation primary-response protein 88 (MyD88) is an essential adapter protein of toll-like receptors (TLRs) except TLR3 in innate immunity and inflammation. Upon response to pathogen-associated molecular patterns (PAMPs), TLRs (except TLR3) recruit MyD88, which results in the activation of mitogen-activated protein kinases (MAPKs) and nuclear factor-κB (NF-κB), leading to the

production of pro-inflammatory cytokines such as TNF-α, IL-1β, and IL-6[5]. MyD88 is also an adaptor protein of interleukin-1 receptor (IL-1R) and plays a central role in IL-1R signaling[6]. Previous studies have indicated that MyD88 deficiency or loss-of-function mutations show anti-inflammatory effect in endotoxin-induced sepsis, arthritis, and autoimmune central nervous system diseases[7–13]. Recently, emerging evidence showed that TLRs, especially TLR2 and TLR4, contribute to diabetic cardiomyopathy through initiating hyperglycemia-induced pro-inflammatory cascades[14, 15]. Inhibition of TLR2 or TLR4 confers significant protection against cardiac remodeling and dysfunction in diabetic mice[16, 17]. However, it is unclear whether MyD88 is necessary for hyperglycemia-induced pro-inflammatory cascades in diabetes-related cardiac injury.

Given that MyD88 is an important adapter protein in TLRs' pro-inflammatory signaling pathways, we speculate that MyD88 may be a potential target for the treatment of diabetic cardiomyopathy. Recently, we identified a series of new small-molecule MyD88 inhibitors. Among them, compound LM8 significantly reduced lipopolysaccharide (LPS)-induced inflammatory cytokine expression in macrophages via directly binding to MyD88 and blocking MyD88-TLR4 complex formation [18]. In this study, we tested the role of MyD88 in diabetic cardiomyopathy using a cardiac specific MyD88 knockout mouse model. The protective roles of MyD88 inhibition in hyperglycemia-induced pro-inflammatory cascades and cardiac injury were further confirmed with MyD88 siRNA and LM8 both *in vivo* and *in vitro*. Our data demonstrate an essential role of cardiomyocyte MyD88 in cardiac inflammation of diabetic mice. Pharmacologic inhibitors of MyD88, e.g., LM8, could be potential therapeutic agents for diabetic cardiomyopathy.

Research Design And Methods

Cell culture

H9c2 and 293T cell-lines were obtained from Cell Bank of Chinese Academy of Sciences (Shanghai, China). Cells were cultured in DMEM containing 1 (for H9c2) or 4.5 g/L (for 293T) glucose, supplemented with 10% heat inactivated FBS, 100 U/ml of penicillin, and 100 mg/ml of streptomycin (Gibco Technologies, Eggenstein, Germany). Primary rat cardiomyocytes and myocardial fibroblasts were isolated from neonatal Sprague-Dawley (SD) rats (0–2 days) and cultured as described previously.[19]

Gene silencing and overexpression

MyD88 silencing in H9c2 cells were performed using 25 nM of rat MyD88 siRNA (siMyD88) (5'-GGAGAUGAUCCGGCAACUATT – 3') or 25nM of scrambled negative control (siNC) siRNA (5'-UUCUCCGAACGUGUCACGUTT-3') (Gene Pharma Co. LTD. Shanghai, China) and Lipofectamine 2000 reagent (Invitrogen, San Diego, CA). After 24 or 48 h of incubation in complete medium, the cells were treated with high-concentration glucose (HG, 33 mM). For MyD88 overexpression, 293T cells were incubated for 6 h in 3 mL OPTI medium containing 9 μg PEI, 1.5μg HA-MyD88, 1.5μg Flag-MyD88 or 3 μg vector control. After 24 h, cells were cultured in complete medium and treated with HG.

Animal experiments

*S*ix-weeks old male C57BL/6N mice (stock # D000274) (18–22 g), male *db/db* mice (BKS$^{db/db}$; stock # T002407) and their male littermate *db/m* (BKS$^{db/m}$) mice, B6/JGpt-MyD88$^{flox/flox}$ mice (stock # T009598), and B6/JGpt-H11$^{Myh6-Cre}$ mice (stock # T004713) were purchased from GemPharmatech Co., Ltd. (Nanjing, China). All mice were housed at a constant room temperature with a 12/12 h light-dark cycle and fed with a standard rodent diet and water in the Animal Centre of Wenzhou Medical University. All animal care and experimental procedures were approved by the Wenzhou Medical University Animal Policy and Welfare Committee.

(1) Type 1 diabetes (T1D) was induced by intraperitoneal injection of 50 mg/kg/day streptozotocin (STZ, from Sigma-Aldrich, dissolved in citrate buffer, pH 4.5) for five days consecutive. Control group received the same volume of citrate buffer. After seven days, fasting blood-glucose levels were measured using glucometer (B. BRAUN, Germany). Mice with fasting glucose levels > 12 mM for three consecutive days were considered diabetic, which were maintained at diabetic status for 16 weeks to induced diabetic cardiomyopathy. Body weight and fasting blood glucose levels were measured weekly for 16 weeks. For LM8 treatment in T1D mice, mice were randomized into non-diabetic controls (Ctrl, n = 7), STZ-induced diabetic mice (STZ, n = 7), diabetic mice treated 5 mg/kg LM8 (STZ + LM8-5), diabetic mice treated 10 mg/kg LM8 (STZ + LM8-10). LM8 (5 and 10 mg/kg) was administered as oral gavage every two days from 9th week to 16th week. The diabetic group and control group received the same volume of 1% CMC-Na solution every two days.

(2) Seven-week-old male *db/db* mice were used as Type 2 diabetes (T2D) model, with littermates *db/m* mice as controls. Mice were maintained at diabetic status for 8 weeks to induced diabetic cardiomyopathy. For LM8 treatment in T2D mice, mice were randomized into *db/m* controls (*db/m*, n = 7), *db/db* diabetic mice (*db/db*, n = 7), diabetic mice treated 5 mg/kg LM8 (*db/db* + LM8-5), diabetic mice treated 10 mg/kg LM8 (*db/db* + LM8-10). LM8 (5 and 10 mg/kg) was administered as oral gavage every two days from 5th week to 8th week. The diabetic group and control group received the same volume of 1% CMC-Na solution every two days. At 7th week in the experiment, intravenous glucose tolerance tests (IGTT) were performed by intraperitoneal injection of glucose (1 g/kg) and subsequent measurement of the blood-glucose levels per 15min using glucometer.

(3) For cardiomyocyte-specific MyD88 knockout study, the cardiomyocyte-specific MyD88 knockout mice (MyD88$^{f/f}$-Myh6^{Cre}) were generated using the *Cre-loxP* method. Mice floxed for MyD88 (MyD88$^{f/f}$) were crossed with mice carrying *Cre-transgene* under the promoter of Myh6 gene (Myh6-Cre) that led to the generation of MyD88$^{f/f}$-Myh6^{Cre} mice. T1D in MyD88$^{f/f}$-Myh6^{Cre} and MyD88$^{f/f}$ mice (7-weeks old) was also induced by intraperitoneal injection of 50 mg/kg/day STZ for five consecutive days (MyD88$^{f/f}$-Myh6^{Cre} + STZ group, n = 7; MyD88$^{f/f}$+STZ group, n = 7). Mice were maintained at diabetic status for 16 weeks to induced diabetic cardiomyopathy. Control MyD88$^{f/f}$-Myh6^{Cre} (n = 7) and MyD88$^{f/f}$ mice (n = 7)

were injected with citrate buffer. Body-weights and fasting glucose levels were measured in all mice weekly for 16 weeks.

At the end of treatment, mice were killed under sodium pentobarbital anesthesia (i.p. injection of 0.2 mL sodium pentobarbital at 100 mg·mL^{-1}). The blood and hearts were collected for subsequent analyses.

Histopathological analyses

Heart tissues were paraffin-embedded and stained with hematoxylin and eosin (H&E) kit (Beyotime, cat. no., C0105S), Masson's Trichrome kit (Solarbio, cat. no. G1340-7) and Sirius Red kit (Solarbio, cat. no. G1471) following the manufacturer's protocol. The stained sections were viewed under a light microscope (Nikon, Japan).

CKMB and LDH activity

Serum creatine kinase MB (CK-MB) and lactate dehydrogenase (LDH) were measured using the Creatine Kinase MB isoenzyme Assay Kit (Cat.no. E006-1-1) and the LDH assay kit (Cat.no. A020-2-2) respectively, following manufacturer's instructions. All kits were obtained from Nanjing Jiancheng Bioengineering Research Institute (Nanjing, China).

Biotin-based pull-down assay

Biotinylated LM8 (Bio-LM8) was synthesized and structurally characterized with a purity of 98.1%. Firstly, 1μM Bio-LM8 was added to 200μl pre-blocked streptavidin-agarose beads and incubated for 1h at room temperature. Biotin and LM8 alone were used as a control. Secondly, lysates prepared from 293T cells that overexpress MyD88 or mouse heart tissues were added to the pre-loading Bio-LM8 streptavidin-agarose beads and then incubated for 4 h at room temperature. Lastly, 50μl 1×SDS loading buffer were added to the bead precipitates to fully elute protein then loaded on SDS-PAGE for immunoblot analysis. Total lysates were used as an input control.

Immunohistochemistry

The deparaffinized and rehydrated sections were treated with boiling 0.01M sodium citrate buffer (pH6.0) to restore antigen and then incubated 3% H_2O_2 for 30 min to block endogenous peroxidase activity. The sections were next blocked with 1% BSA in PBS for 30 min, incubated at 4°C overnight with the TNF-α primary antibody (Santa, cat.no. SC52746 1:200 dilution) followed by incubation for 1 h with HRP-conjugated secondary antibodies (1:500 dilution) and then immunoreactivity was detected by diaminobenzidine (DAB) following the manufacturer's protocol. The stained sections were viewed under a light microscope (Nikon, Japan).

Immunofluorescence

The immobilized and permeabilized sections were incubated with primary antibody anti-MyD88 (CST, Cat.no. 9252), anti-α-actin (abcam, Cat.no. ab9465), anti-vimentin (abcam, Cat.no. ab8978) or anti-p65 (CST, Cat.no. 8242) and then subsequently fluorescence probe labeled secondary antibodies (abcam,

Goat Anti-Mouse IgG-TRITC, Cat.no. ab6786; Goat Anti-rabbit IgG-TRITC, Cat.no. ab6718; or Goat Anti-rabbit IgG-Fluor® 488, Cat.no. ab150077) after blocking according the manufacturer's protocol. For of phalloidine- DyLight™ 554 staining, the immobilized and permeabilized cells were incubated with 1μg/ml phalloidine- DyLight™ 554 (CST, Cat.no. 13054) in a humidified chamber at 37°C for 30 mins. DAPI (CST, Cat.no. 4083) was used for counterstaining nucleus. The stained sections were viewed under a fluorescence microscope (Nikon, Japan).

Immunoblotting and immunoprecipitation

Antibodies for GAPDH (sc-365062), β-Actin (sc-47778), MyD88 (sc-74532), TLR4 (sc-293072), TGF-β (sc-130348), Collagen-I (sc-59772), p-ERK1/2 (sc-81492), ERK1/2 (sc-514302), IκBα (sc-1643), Flag (sc-166384), HA (sc-7392), MyHC (sc-376157), Lamin B1 (sc-374015) were obtained from Santa Cruz Biotechnology (Santa Cruz, CA). Antibody for Flag (DYKDDDDK Tag, cat. no. 14793), TLR2 (cat. no. 12276), JNK (cat. no. 9252), p-JNK (cat. no. 9255) were obtained from Cell Signaling Technology (Danvers, MA). Total proteins from cells or homogenized tissues were extracted using RIPA lysis buffer (Beyotime Biotech., Nanjing, China). Nuclear and cytoplasmic proteins were isolated using kit following manufacturer's instructions (Beyotime Biotech., Nanjing, China). Protein complexes were evaluated by co-immunoprecipitation followed with immunoblotting. Briefly, cells or heart tissues were lysed with lysis buffer containing 50 mM Tris-HCl pH 7.4, 150 mM NaCl, 1% Triton-X 100, 1% Sodium Deoxycholate. Protein samples (500–1000 μg) were incubated with precipitating antibody at 4°C overnight, and immunoprecipitated with protein A + G-Sepharose beads at room temperature for 2 h. The protein-bead complexes were washed 5-times with PBS, then 50 μl 1x SDS loading buffer were added to protein-bead complexes and then loaded on SDS-PAGE for immunoblot analysis. Immunoreactivity was visualized using an enhanced chemiluminescence reagents and quantified using Image J analysis software version 1.38e (NIH, Bethesda, USA). Values were normalized to loading controls.

Real-time quantitative PCR

Total RNAs were extracted from cells or tissues using TRIZOL (Invitrogen). Reverse transcription and quantitative PCR (qPCR) were carried out using PrimeScript™ RT reagent Kit and SYBR premix taqII (Takara). Bio-Rad CFX96 real time system (Bio-Rad Tech., Shanghai, China) was used for qPCR analysis using standard protocols. The primer sequences of target genes are listed in the supplementary Table S1 (Invitrogen). The amount of each gene was normalized to the amount of β-actin. For genomic PCR, genomic DNA were extracted from the toe of the mice (3 weeks old) using protease K digestion and saturated NaCl sedimentation and then PCR was performed. The primer sequences of target DNA fragment are listed in Table S2 (Invitrogen). Following electrophoresis, PCR products were visualized on 2% agarose gel containing 0.5 μg/mL SYBR.

Statistical analysis

All experiments were randomized. *In-vitro* experiments were repeated at least 3 times. Data are presented as Means ± SEMs. The statistical significance of differences between groups was obtained by the student's t-test or ANOVA multiple comparisons in GraphPad Pro8.0 (GraphPad, San Diego, CA). We used

one-way ANOVA followed by Dunnett's post-hoc test when comparing more than two groups and one-way ANOVA, non-parametric Kruskal–Wallis test followed by Dunn's post-hoc test when comparing multiple independent groups. $P < 0.05$ was considered statistical significance.

Results

MyD88 expression was upregulated in the cardiomyocytes of diabetic mice

Firstly, we measured the expression level of MyD88 in T1D mouse hearts. Western blot analysis showed that MyD88 expression was significantly increased in the hearts of STZ-induced T1D mice compared to the non-diabetic controls (Fig. 1A). The same changes in TLR2 and TLR4 proteins were observed in hearts of T1D mice (Fig. 1A). Interestingly, immunoprecipitation assay of heart tissue lysates revealed increased MyD88 interaction with TLR2 and TLR4 (Fig. 1B), further indicating an activated state of MyD88 in diabetic hearts. To confirm the source of increased MyD88 expression, we performed immunofluorescence in mouse heart sections using doubly-staining for MyD88 and either cardiomyocyte-specific marker actin or fibroblast-specific marker vimentin.[14] Our double-staining immunofluorescence and quantification data indicated significantly increased expression and co-localization of MyD88 mainly in the cardiomyocytes of diabetic mice (Fig. 1C, 1E). Comparatively, a faint expression level of MyD88 was observed in the cardiac fibroblasts of STZ-treated mice and control mice (Fig. 1D, 1E). Immunofluorescence data was further validated by measuring MyD88 expression in rat primary cardiomyocytes and primary cardiac fibroblasts by immunoblotting. The result confirmed a much higher expression in cardiomyocytes in comparison to fibroblasts (Fig. 1F). We then treated the primary cardiomyocytes with HG at 33mM. As shown in Fig. 1G and supplementary Figure S1A, HG challenge for a long time (24 or 48 h) induced MyD88 expression. However, HG stimulation for 25 or 30 min significantly activated MyD88, evidenced by increased MyD88 interaction with TLR2 and TLR4 in primary cardiomyocytes (Fig. 1H). This induction was not seen in 33mM mannitol-challenged H9c2 cells, indicating osmotic stress is not involved in MyD88 activation (supplementary Figure S1B). These data show that diabetes/HG could up-regulate and activate MyD88 in cardiomyocytes, indicating the involvement of MyD88 in diabetic cardiomyopathy.

Cardiomyocyte-specific MyD88 knockout prevented STZ-induced cardiac inflammation and injury

To investigate the role of MyD88 in the hearts of T1D mice, cardiomyocyte-specific MyD88 knockout mice were generated by crossing $Myh6^{Cre}$ and $MyD88^{f/f}$ mice (Supplementary Figure S2A-B). Successful cardiac MyD88 deletion was validated by western blot in the isolated adult mouse cardiomyocytes (Supplementary Figure S2C). As shown in Fig. 2A, cardiac MyD88 deletion did not affect hyperglycemia induced by STZ. Similarly, cardiac MyD88 deletion also had no effect on the body weight of both healthy and T1D mice (Fig. 2B). Interestingly, the heart weight/tibia length (HW/TL) ratio was significantly increased in STZ-treated $MyD88^{f/f}$ mice, and cardiac MyD88 deletion completely prevented this increase

(Fig. 2C). Moreover, plasma lactate dehydrogenase (LDH) and creatine kinase isoenzyme-MB (CK-MB), two biochemical indices of myocardial injury, were increased in STZ-treated MyD88$^{f/f}$ mice, and cardiac MyD88 deletion blunted these increases (Fig. 2D-E). H&E staining was performed on transverse and longitudinal heart sections, which show increased structural abnormalities and increased cardiomyocyte area, indicating cardiac hypertrophy in the hearts of STZ-treated mice in comparison to control mice. However, the increased cardiomyocyte area was completely prevented in STZ-treated MyD88-deficient mice (Fig. 2F and supplementary Figure S3A). Masson's trichrome and Sirius red staining analysis showed increased collagen deposition in the hearts of STZ-treated MyD88$^{f/f}$ mice, which was also prevented by cardiac MyD88 deletion (Fig. 2G and supplementary Figure S3B-C). Further western blot and qPCR analyses on the heart tissues showed significant increases of MyHc, Col-I and TGF-β expression in STZ-treated MyD88$^{f/f}$ mice, and these hypertrophic and fibrotic responses were completely prevented by cardiac MyD88 deletion (Fig. 2H-I and supplementary Figure S3D).

We then examined inflammatory cascades and cytokine expression in heart tissues. MAPK pathways, i.e., p-ERK and p-JNK, were activated and IκB-α was reduced in STZ-treated MyD88$^{f/f}$ mice, indicating MAPKs and NF-κB activation. (Fig. 2J and supplementary Figure S3E). Subsequently, gene expression levels of TNF-α, IL-6, and IL-1β were significantly increased in STZ-treated MyD88$^{f/f}$ mice (Fig. 2K). Importantly, MAPKs activation, IκB-α degradation, and increased expression of proinflammatory cytokines were markedly prevented by cardiac MyD88 deletion (Fig. 2J-K and supplementary Figure S3E).

MyD88 knockdown attenuated HG-induced inflammation and fibrosis in cultured cardiomyocytes

To confirm the *in vivo* role of MyD88 in diabetic cardiomyopathy, rat cardiomyocyte-like H9c2 cells were transfected with MyD88 siRNA (siMyD88), and then treated with high glucose (HG, 33 mM). Our group has previously reported that 33mM mannitol does not induce inflammatory response in H9c2 cells, which excluded the pro-inflammatory effect of high osmotic condition[14]. MyD88 knockdown was confirmed by western blot (Fig. 3A). As expected, HG markedly increased p-ERK and p-JNK levels, reduced IκB-α level, and promoted P65 nuclear translocation, while MyD88 knockdown clearly prevented HG-induced MAPKs and NF-κB activation (Fig. 3B-C and supplementary Figure S4A-B). As a result, MyD88 knockdown significantly prevented HG-induced expression of proinflammatory cytokines (TNF-α, IL-6, and IL-1β, in Fig. 3D) and hypertrophic and profibrotic genes (MyHc, Col-1, and TGF-β) (Fig. 3E-F and supplementary Figure S4C).

Pharmacological inhibition of MyD88 by LM8 suppresses HG-induced inflammation and hypertrophy in cardiomyocytes

The chemical structure of MyD88 inhibitor LM8 was shown (Fig. 4A). We previously demonstrated that LM8 inhibited MyD88-mediated inflammation by preventing its dimerization in macrophages.[18, 20] A biotinylated LM8 (Bio-LM8, in the supplementary Figure S5A), which showed same anti-inflammatory

effects compared to LM8 (supplementary Figure S5B), was used for further target validation in cells and heart tissues. Successful binding of LM8 to MyD88 protein was observed in 293T cells and mouse heart tissues by using biotinylated protein interaction pull-down assays (supplementary Figure S5C-D). We then confirmed that HG induced MyD88 dimerization and MyD88-TLR4 complex formation in H9c2 cells, which were prevented by LM8 treatment (Fig. 4B-C and supplementary Figure S6A-B). Subsequently, western blot assay examined HG-induced phosphorylation of ERK and JNK, as well as IκB degradation and P65 nuclear translocation in H9c2 cells, while this HG-induced activation of MAPKs and NF-κB signaling was significantly prevented with LM8 treatment at 2.5, 5 and 10 μM (Fig. 4D and supplementary Figure S6C). LM8 treatment dose-dependently inhibited HG-induced P65 nuclear translocation, which was further confirmed by immunofluorescence staining in H9c2 cells (Fig. 4E-F). As a result, HG-induced expression of inflammatory cytokines, including TNF-α, IL-6, and IL-1β, were significantly reduced by LM8 treatment dose-dependently (Fig. 4G).

Next, we tested the effect of LM8 on HG-induced hypertrophic and fibrotic responses. HG significantly increased cell sizes determined by rhodamine phalloidine staining, and LM8 treatment dose-dependently (2.5, 5 and 10 μM) reduced the cell sizes (Fig. 4H-I). Meanwhile, HG-induced expression of MyHc, Col-1, and TGF-β was significantly reduced by LM8 treatment (Fig. 4J-K and supplementary Figure S6D). We validated the protective effects LM8 in rat primary cardiomyocytes. Similarly, HG induced significant activation of MAPKs and NF-κB pathways, upregulation of TNF-α, IL-6, IL-1β, MyHc, Col-1, and TGF-β in rat primary cardiomyocytes, and these HG-induced effects were significantly blunted by LM8 (10 μM) treatment (Figure S7A-E). Taken together, MyD88 inhibition by LM8 protects against HG-induced inflammation and hypertrophy in cardiomyocytes *via* inhibiting MyD88-TLR4 complex formation and subsequent activation of MAPKs and NF-κB.

LM8 prevented cardiac inflammation and injury in mouse T1D model

Next, the therapeutic effect of MyD88 inhibition by LM8 was tested in mouse T1D model. The administration doses of LM8 at 5 and 10 mg/kg were chosen according to previous studies.[18, 21] LM8 treatment did not affect blood glucose level and body weight in T1D mice (Fig. 5A-B). Similar to the results of cardiac MyD88 knockout, LM8 treatment at both doses significantly decreased HW/TL ratio, serum LDH and CK-MB activity in T1D mice compared to the vehicle treated T1D mice (Fig. 5C-E). H&E staining of transverse and longitudinal heart sections demonstrated improvement of T1D-induced cardiac hypertrophy and structural abnormality with LM8 treatment (Fig. 5F and supplementary Figure S8A). LM8 treatment also reduced T1D-induced cardiac fibrosis evidenced by reduced Masson's trichrome and Sirius red staining (Fig. 5G and supplementary Figure S8B-C). LM8 administration also dose-dependently reduced the expression levels of MyHc, Col-I, and TGF-β in the hearts of T1D mice (Fig. 5H-I and supplementary Figure S8D). Parallelly, LM8 treatment diminished T1D-induced activation of ERK and JNK and IκB-α degradation in diabetic hearts (Fig. 5J and supplementary Figure S8E). Real-time qPCR assay showed dose-dependent inhibition of LM8 against diabetes-induced production of inflammatory cytokines TNF-α, IL-6, and IL-1β in heart tissues (Fig. 5K and supplementary Figure S8F-G).

Of note, MyD88-TLR4 complex formation was clearly increased in the hearts of T1D mice, which was markedly blocked by LM8 treatment (Fig. 5L and supplementary Figure S8H). Overall, this data demonstrates that LM8 treatment protects hearts against diabetes-induced cardiac injury by inhibiting MyD88-mediated inflammation rather than reducing hyperglycemia in T1D mice.

LM8 prevented cardiac inflammation and injury in db/db mice

To further validate the protective effect of LM8 on diabetic cardiomyopathy, *db/db* mice were used to produce T2D mouse model. Seven-week-old *db/db* and *db/m* control mice were treated with LM8 at 5 and 10 mg/kg for the last 4 weeks. We also saw that MyD88 was over-expressed in hearts of *db/db* mice, compared to *db/m* mice (supplementary Figure S9). LM8-treatment did not affect blood glucose and body weight in *db/db* mice (Fig. 6A-B). LM8-treatment also did not improve insulin resistance in *db/db* mice, evidenced by IGTT and ITT assay (supplementary Figure S10A-B). Like the results in T1D mice, increased HW/BW ratio and serum CK-MB and LDH levels in *db/db* mice were significantly inhibited by LM8-treatment (Fig. 6C-E). H&E staining analysis showed that LM8 attenuated cardiac hypertrophy and pathological changes in *db/db* mice (Fig. 6F and supplementary Figure S11A). Sirius red and Masson's trichrome staining showed that LM8 treatment also significantly reduced fibrosis in *db/db* mice heart sections (Fig. 6G and supplementary Figure S11B-C). LM8 administration also reduced the expression levels of MyHc, Col-I, and TGF-β in the hearts of *db/db* mice (Fig. 6H-I and supplementary Figure S11D). Parallelly, LM8 treatment diminished activation of ERK, JNK, and NF-κB (Fig. 6J and supplementary Figure S11E) and production of inflammatory cytokines TNF-α, IL-6, and IL-1β (Fig. 6K) in the hearts of *db/db* mice. Similarly, LM8-treatment inhibited MyD88-TLR4 complex formation in the hearts of *db/db* mice (Fig. 6L and supplementary Figure S11F). Overall, our data in *db/db* mice show that LM8 protects the heart by inhibiting cardiac inflammation without affecting hyperglycemia or insulin resistance in T2D mouse models. Taken together, this data demonstrates that LM8 treatment protects diabetic hearts by inhibiting MyD88-mediated inflammation rather than reducing hyperglycemia or improvement of insulin resistance in the T2D mouse model.

Discussion

Our results showed that MyD88 expression and activity were increased in the cardiomyocytes of diabetic mice. HG treatment significantly increased MyD88-TLR4 interaction, activated MAPKs and NF-κB signaling, and induced proinflammatory and profibrotic responses in cultured cardiomyocytes, and MyD88 inhibition with LM8 or siRNA markedly prevented these HG-induced changes *in vitro*. Importantly, cardiomyocyte-specific MyD88 gene knockout significantly ameliorated hyperglycemia-induced activation of MAPKs and NF-κB and reduced subsequently inflammatory injury and remodeling in the hearts of T1D mice. These protective roles were further confirmed by the fact that LM8 treatment prevented cardiac inflammation and injury, pathological remodeling and fibrosis in both STZ-treated mice and *db/db* mice. As summarized in Fig. 7, these results shed new light on the role of MyD88 in inflammatory diabetic cardiomyopathy and provide a mechanistic basis for diabetes/HG-induced cardiac

inflammation. This study also indicates that pharmacologic inhibitors of MyD88 could be potential therapeutic agents for diabetic cardiomyopathy.

Myocardial inflammation and fibrosis are two key pathophysiological mechanisms that drive cardiac remodeling and dysfunction resulting in heart failure.[22] Epidemiological studies suggest that hyperglycemia, a hallmark of either T1D or T2D, is closely associated with a chronic low-level inflammation that contributes to myocardial damage, leading to diabetic cardiomyopathy.[23] Given the central role of inflammation in the progress of diabetic cardiomyopathy, several anti-inflammatory drugs-based approaches have shown therapeutic effects on diabetic cardiomyopathy.[24] However, there are currently no drugs or therapies available to improve cardiac fibrosis in diabetic cardiomyopathy. In the current study, MyD88 inhibition significantly improved cardiac injury and reduced cardiac inflammation and fibrosis in T1D and T2D mouse models. It is interesting that neither genetic nor pharmacologic inhibition of MyD88 affected hyperglycemia in mice with T1D or T2D, indicating that the cardiac benefits observed in T1D and T2D mice were mainly due to the anti-inflammatory effect of MyD88 inhibition.

Activation of TLRs has been associated with increased susceptibility to diabetic vascular complications, nephropathy, cardiomyopathy, retinopathy, and neuropathy [25]. In diabetic mice, activation of TLR2 or 4 is associated with increased production of proinflammatory cytokines, pro-fibrotic molecules, pro-apoptotic markers, as well as cardiac dysfunction through binding to MyD88.[26–30] TLR3 and TLR6 has also been reported to promote high glucose-induced cardiomyocyte apoptosis[31] and NF-κB signaling, respectively.[28] Following recruitment to TLRs except TLR3, MyD88 interacts with IRAK2/4 (Interleukin 1 Receptor Associated Kinase 2/4) through the death domains and leads to the activation of NF-κB and MAPKs (mainly ERK and JNK pathways) and subsequent expression of pro-inflammatory cytokines.[5, 32] Given that several TLRs are involved in the pathogenesis of diabetic cardiomyopathy, inhibition of MyD88, a molecular target downstream to TLRs, may be a more appropriate strategy that antagonism of certain TLR. For instance, TLR4 antagonists could not block inflammation mediated by other TLRs, which may be a main reason for the failure of TLR4 antagonists, eritoran and TAK-242, in clinical efficiency of sepsis therapy [33]. In this study, increased MyD88-TLR2/4 interaction was confirmed in the hearts of diabetes mice, accompanied with activation of MAPKs and NF-κB resulting in increased cardiac inflammatory and fibrotic responses, and these were prevented by either genetic or pharmacological MyD88 inhibition. In addition, MyD88 is expressed in the heart, liver, spleen, lungs, kidney, thymus, lymph nodes and digestive systems at different developmental stages, indicating its important role. [34] However, the systemic MyD88 knockout mice were viable without any overt phenotype, [7] indicating that MyD88 is dispensable physiologically and strategies to inhibit MyD88 at any stage of life are expected not to show strong side-effects in other cell-type or organ systems. This study validates this deduction by good efficiency and high safety of LM8 in both type 1 and type 2 diabetic mice. These data demonstrate that MyD88 is a promising target to treat diabetic cardiomyopathy.

TLR2 and TLR4 were expressed in cardiomyocytes[17, 28, 35] and cardiac fibroblasts[36] in hearts. As TLRs adaptor protein, MyD88 expression is found in the heart, but its expression distribution and function in cardiomyocytes, particularly in the diabetic setting, remain unknown. Our data, for the first time,

demonstrate that MyD88 predominantly expressed in cardiomyocytes in hearts. MyD88 expression and its interaction with TLR2 and TLR4 were increased in cardiomyocytes in the setting of high glucose or diabetes. Cardiomyocyte-specific MyD88 knockout mice demonstrated that MyD88-deficiency protected cardiomyocytes against hyperglycemia-induced cardiac inflammation and injury via reducing MAPKs and NF-κB activation. Cardiac fibroblasts are also important in the progression of diabetic cardiomyopathy [37, 38]. However, our data showed a strong induction of MyD88 only in the cardiomyocyte by diabetes and then cardiac protective effects following the cardiomyocyte-specific loss of MyD88, indicating a relatively robust role played by cardiomyocytes than cardiac fibroblasts. It is also important to note that LM8 was systemically delivered to inhibit MyD88 in every cell-type, but we did not observe an additive protective effect of LM8 in comparison to genetic inhibition of cardiomyocyte MyD88. This also indicates that cardiomyocyte MyD88 plays a key role in diabetic cardiomyopathy in comparison to cardiac fibroblasts. However, a limitation of this study may be the absence of the evaluation of infiltrated macrophages in heart. Given that infiltrated macrophages contribute to diabetic cardiac inflammation [14], it should be necessary in the future to examine whether MyD88 in macrophages also contributes to cardiac inflammatory injuries in diabetes.

This study indicates that strategies aiming to inhibit MyD88 in cardiomyocytes may be a potential therapeutic approach for diabetic cardiomyopathy. However, there are some limitations of the study. First, only cardiac injury/remodeling was evaluated in the mice, and cardiac function was not assessed that is more important in clinic setting and needs to be further investigated in future studies. Second, only the classic and known MAPKs/NF-κB pathways associated with MyD88 signalling were analysed in this study, therefore, a global pathway analysis, especially after MyD88 inhibition, would be valuable to explore the underlying mechanisms and potential safety issues.

Conclusion

In our study demonstrates that cardiomyocyte MyD88 mediates inflammatory diabetic cardiomyopathy via MyD88-MAPKs/NF-κB pro-inflammatory signalling pathway. Genetic and pharmacologic inhibition of MyD88 showed significantly cardioprotective effects on hyperglycemia-induced inflammation and fibrosis *in-vitro* and *in-vivo,* indicating that pharmacologic inhibitors of MyD88 could be potential therapeutic agents for diabetic cardiomyopathy.

Abbreviations

Bio-LM8, Biotinylated LM8; CK-MB, creatine kinase type M/B; CMC-Na, Carboxymethylcellulose sodium; Col-I, type 1 Collagen; DAB, diaminobenzidine; DAPI, 4'6-diamidino-2-phenylindole; ERK1/2, extracellular regulated protein kinases1/2; GAPDH, glyceraldehyde-3-phosphate dehydrogenase; HG, high glucose; HW/TL, heart weight/tibia length; IGTT, intravenous glucose tolerance tests; IL-1β, interleukins 1b (IL-1β); IL-1R, interleukin-1 receptor; IL-6, interleukins 6; IRAK2/4, Interleukin 1 Receptor Associated Kinase 2/4; ITT, insulin tolerance tests; IκBα, I-kappa-B-alpha; JNK, c-Jun N-terminal kinase, stress-activated protein kinase; LPS, lipopolysaccharide; MAPKs, mitogen-activated protein kinases; MyD88, Myeloid

differentiation primary-response protein 88; Myh6, Myosin heavy chain 6; MyHC, Myosin heavy chain, cardiac muscle; NF-κB, nuclear factor-κB; PAMPs, pathogen-associated molecular patterns; PBS, phosphate buffered solution; PCR, Quantitative Polymerase Chain Reaction; PEI, Polyetherimide; SDS-PAGE, sodium dodecyl sulfate polyacrylamide gel electrophoresis; STZ, streptozotocin; T1D, type 1 diabetes; T2D, type 2 diabetes; TGF-β, Transforming growth factor-beta; TLR, Toll-like receptor; TNF-α, tumor necrosis factor α; TRITC, tetraethyl rhodamine isothiocyanate.

Declarations

Acknowledgements

None

Author Contributions

G.L., Y.W., and W.L. contributed to the literature search and study design. G.L. and G.W. participated in the drafting of the article. W.L., X.C., Q.Z., C.Z., and J.L. carried out the experiments. Y.W., N.C., and G.W. revised the manuscript. G.W. and W.L. contributed to data collection and analysis.

Funding

This study was supported by the National Key Research Project (2017YFA0506000 to G.L.), National Natural Science Foundation of China (82000793 to W.L., 81770825 to G.L.), Thailand Research Found Grant (DBG6280006 to N.C.), Natural Science Foundation of Zhejiang Province (LY19H020004 to G.W.), Zhejiang Provincial Key Scientific Project (2021C03041 and 2018C03068 to G.L.), and Wenzhou Science and Technology Key Project (2018ZY009 to G.L.).

Availability of data and materials

The datasets used and/or analyzed during the current study are available from the corresponding author on reasonable request.

Ethics approval and consent to participate

This study was approved by the Wenzhou Medical University Animal Policy and Welfare Committee.

Consent of publication

Not applicable.

Competing interests

All the authors declare no competing interest.

References

1. Kannel WB, Hjortland M, Castelli WP. Role of diabetes in congestive heart failure: the Framingham study. Am J Cardiol. 1974;34(1):29–34.
2. Jia G, Hill MA, Sowers JR. Diabetic Cardiomyopathy: An Update of Mechanisms Contributing to This Clinical Entity. Circ Res. 2018;122(4):624–38.
3. Tsalamandris S, Antonopoulos AS, Oikonomou E, Papamikroulis GA, Vogiatzi G, Papaioannou S, Deftereos S, Tousoulis D. The Role of Inflammation in Diabetes: Current Concepts and Future Perspectives. Eur Cardiol. 2019;14(1):50–9.
4. Jia G, DeMarco VG, Sowers JR. Insulin resistance and hyperinsulinaemia in diabetic cardiomyopathy. Nat Rev Endocrinol. 2016;12(3):144–53.
5. Gay NJ, Symmons MF, Gangloff M, Bryant CE. Assembly and localization of Toll-like receptor signalling complexes. Nat Rev Immunol. 2014;14(8):546–58.
6. Chen L, Zheng L, Chen P, Liang G. Myeloid Differentiation Primary Response Protein 88 (MyD88): The Central Hub of TLR/IL-1R Signaling. J Med Chem. 2020;63(22):13316–29.
7. Kawai T, Adachi O, Ogawa T, Takeda K, Akira S. Unresponsiveness of MyD88-deficient mice to endotoxin. Immunity. 1999;11(1):115–22.
8. Kiripolsky J, Kasperek EM, Zhu C, Li QZ, Wang J, Yu G, Kramer JM. Tissue-specific activation of Myd88-dependent pathways governs disease severity in primary Sjogren's syndrome. J Autoimmun. 2021;118:102608.
9. Kader M, Alaoui-El-Azher M, Vorhauer J, Kode BB, Wells JZ, Stolz D, Michalopoulos G, Wells A, Scott M, Ismail N. MyD88-dependent inflammasome activation and autophagy inhibition contributes to Ehrlichia-induced liver injury and toxic shock. PLoS Pathog. 2017;13(10):e1006644.
10. Chen CJ, Shi Y, Hearn A, Fitzgerald K, Golenbock D, Reed G, Akira S, Rock KL. MyD88-dependent IL-1 receptor signaling is essential for gouty inflammation stimulated by monosodium urate crystals. J Clin Invest. 2006;116(8):2262–71.
11. Sikora KA, Bennett JR, Vyncke L, Deng Z, Tsai WL, Pauwels E, Layh-Schmitt G, Brundidge A, Navid F, Zaal KJM, et al: **Germline gain-of-function myeloid differentiation primary response gene-88 (MYD88) mutation in a child with severe arthritis**. *J Allergy Clin Immunol* 2018, **141**(5):1943–1947 e1949.
12. Zheng C, Chen J, Chu F, Zhu J, Jin T. Inflammatory Role of TLR-MyD88 Signaling in Multiple Sclerosis. Front Mol Neurosci. 2019;12:314.
13. Rangasamy SB, Jana M, Roy A, Corbett GT, Kundu M, Chandra S, Mondal S, Dasarathi S, Mufson EJ, Mishra RK, et al. Selective disruption of TLR2-MyD88 interaction inhibits inflammation and

attenuates Alzheimer's pathology. J Clin Invest. 2018;128(10):4297–312.

14. Wang Y, Luo W, Han J, Khan ZA, Fang Q, Jin Y, Chen X, Zhang Y, Wang M, Qian J, et al. MD2 activation by direct AGE interaction drives inflammatory diabetic cardiomyopathy. Nat Commun. 2020;11(1):2148.
15. Dasu MR, Devaraj S, Zhao L, Hwang DH, Jialal I. High glucose induces toll-like receptor expression in human monocytes: mechanism of activation. Diabetes. 2008;57(11):3090–8.
16. Zhang Y, Li Y, Huang X, Zhang F, Tang L, Xu S, Liu Y, Tong N, Min W. Systemic Delivery of siRNA Specific for Silencing TLR4 Gene Expression Reduces Diabetic Cardiomyopathy in a Mouse Model of Streptozotocin-Induced Type 1 Diabetes. Diabetes Ther. 2020;11(5):1161–73.
17. Zhang Y, Peng T, Zhu H, Zheng X, Zhang X, Jiang N, Cheng X, Lai X, Shunnar A, Singh M, et al. Prevention of hyperglycemia-induced myocardial apoptosis by gene silencing of Toll-like receptor-4. J Transl Med. 2010;8:133.
18. Chen L, Chen H, Chen P, Zhang W, Wu C, Sun C, Luo W, Zheng L, Liu Z, Liang G. Development of 2-amino-4-phenylthiazole analogues to disrupt myeloid differentiation factor 88 and prevent inflammatory responses in acute lung injury. Eur J Med Chem. 2019;161:22–38.
19. Wang Y, Qian Y, Fang Q, Zhong P, Li W, Wang L, Fu W, Zhang Y, Xu Z, Li X, et al. Saturated palmitic acid induces myocardial inflammatory injuries through direct binding to TLR4 accessory protein MD2. Nat Commun. 2017;8:13997.
20. Singh S, Adam M, Matkar PN, Bugyei-Twum A, Desjardins JF, Chen HH, Nguyen H, Bazinet H, Michels D, Liu Z, et al. Endothelial-specific Loss of IFT88 Promotes Endothelial-to-Mesenchymal Transition and Exacerbates Bleomycin-induced Pulmonary Fibrosis. Sci rep. 2020;10(1):4466.
21. Ferguson F, Nabet B, Raghavan S, Liu Y, Leggett A, Kuljanin M, Kalekar R, Yang A, He S, Wang J, et al. Discovery of a selective inhibitor of doublecortin like kinase 1. Nat chem biol. 2020;16(6):635–43.
22. Suthahar N, Meijers WC, Sillje HHW, de Boer RA. From Inflammation to Fibrosis-Molecular and Cellular Mechanisms of Myocardial Tissue Remodelling and Perspectives on Differential Treatment Opportunities. Curr Heart Fail Rep. 2017;14(4):235–50.
23. Pickup JC, Mattock MB, Chusney GD, Burt D. NIDDM as a disease of the innate immune system: association of acute-phase reactants and interleukin-6 with metabolic syndrome X. Diabetologia. 1997;40(11):1286–92.
24. Filardi T, Ghinassi B, Di Baldassarre A, Tanzilli G, Morano S, Lenzi A, Basili S, Crescioli C. **Cardiomyopathy Associated with Diabetes: The Central Role of the Cardiomyocyte**. *Int J Mol Sci* 2019, 20(13).
25. Wang X, Antony V, Wang Y, Wu G, Liang G. Pattern recognition receptor-mediated inflammation in diabetic vascular complications. Med Res Rev. 2020;40(6):2466–84.
26. Monnerat G, Alarcon ML, Vasconcellos LR, Hochman-Mendez C, Brasil G, Bassani RA, Casis O, Malan D, Travassos LH, Sepulveda M, et al. Macrophage-dependent IL-1beta production induces cardiac arrhythmias in diabetic mice. Nat Commun. 2016;7:13344.

27. Lei L, Hu H, Lei Y, Feng J. Leukocytic toll-like receptor 2 knockout protects against diabetes-induced cardiac dysfunction. Biochem Biophys Res Commun. 2018;506(3):668–73.
28. Dong B, Qi D, Yang L, Huang Y, Xiao X, Tai N, Wen L, Wong FS. TLR4 regulates cardiac lipid accumulation and diabetic heart disease in the nonobese diabetic mouse model of type 1 diabetes. Am J Physiol Heart Circ Physiol. 2012;303(6):H732–42.
29. Zhenzhong Z, Yafa Y, Jin L. **Fibrinogen-like protein 2 gene silencing inhibits cardiomyocytes apoptosis, improves heart function of streptozotocin-induced diabetes rats and the molecular mechanism involved**. *Biosci Rep* 2015, 35(3).
30. Zhang X, Pan L, Yang K, Fu Y, Liu Y, Chi J, Zhang X, Hong S, Ma X, Yin X. H3 Relaxin Protects Against Myocardial Injury in Experimental Diabetic Cardiomyopathy by Inhibiting Myocardial Apoptosis, Fibrosis and Inflammation. Cellr physiol biochem. 2017;43(4):1311–24.
31. Liu Q, Zhang J, Xu Y, Huang Y, Wu C. Effect of carvedilol on cardiomyocyte apoptosis in a rat model of myocardial infarction: a role for toll-like receptor 4. Indian J Pharmacol. 2013;45(5):458–63.
32. Lim MX, Png CW, Tay CY, Teo JD, Jiao H, Lehming N, Tan KS, Zhang Y. Differential regulation of proinflammatory cytokine expression by mitogen-activated protein kinases in macrophages in response to intestinal parasite infection. Infect Immun. 2014;82(11):4789–801.
33. Rice TW, Wheeler AP, Bernard GR, Vincent JL, Angus DC, Aikawa N, Demeyer I, Sainati S, Amlot N, Cao C, et al. A randomized, double-blind, placebo-controlled trial of TAK-242 for the treatment of severe sepsis. Crit Care Med. 2010;38(8):1685–94.
34. Gan L, Qin W, Wu S, Wu S, Bao W. Spatiotemporal expression of MYD88 gene in pigs from birth to adulthood. Genet Mol Biol. 2018;41(1):119–24.
35. Liu ZW, Wang JK, Qiu C, Guan GC, Liu XH, Li SJ, Deng ZR. Matrine pretreatment improves cardiac function in rats with diabetic cardiomyopathy via suppressing ROS/TLR-4 signaling pathway. Acta Pharmacol Sin. 2015;36(3):323–33.
36. Tao A, Song J, Lan T, Xu X, Kvietys P, Kao R, Martin C, Rui T. Cardiomyocyte-fibroblast interaction contributes to diabetic cardiomyopathy in mice: Role of HMGB1/TLR4/IL-33 axis. Biochim Biophys Acta. 2015;1852(10 Pt A):2075–85.
37. Russo I, Frangogiannis NG. Diabetes-associated cardiac fibrosis: Cellular effectors, molecular mechanisms and therapeutic opportunities. J Mol Cell Cardiol. 2016;90:84–93.
38. Levick SP, Widiapradja A. **The Diabetic Cardiac Fibroblast: Mechanisms Underlying Phenotype and Function**. *Int J Mol Sci* 2020, 21(3).

Figures

Figure 1

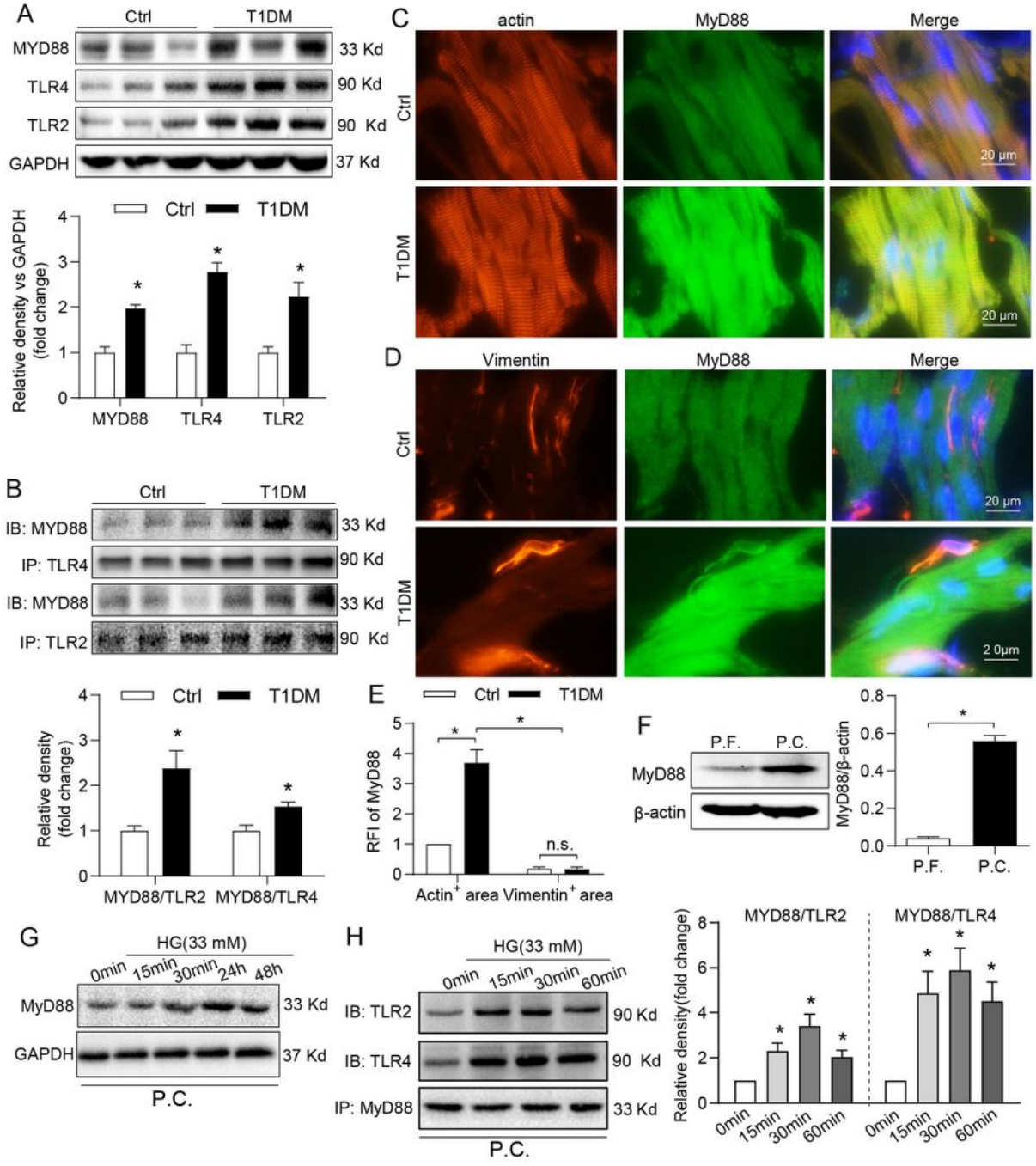

Figure 1

MyD88 expression was up-regulated in cardiomyocytes of diabetic mice. (A) Protein levels of TLR4, TLR2 and MyD88 were detected by western blot assay in heart tissue lysates of STZ-induced T1D and control (ctrl) mice; GAPDH was loading control. Densitometric quantification was shown below. (B) Protein interactions of TLR4-MyD88 and TLR2-MyD88 were analyzed using Co-IP assay in heart tissues of T1D and ctrl mice. Densitometric quantification was shown below. (C) Representative images of the

immunofluorescent double-staining for MyD88 (green) and cardiomyocyte-marker actin (orange). (D) Representative images of the immunofluorescent double-staining for MyD88 (green) and fibroblast-marker vimentin (orange). (E) Quantification for panel C and D, shown by the relative fluorescence intensity (RFI) fold compared to the MyD88-positive area. (F) Western blot analysis for MyD88 protein in primary myocardial fibroblasts (P.F.) and primary cardiomyocytes (P.C.) of neonatal rats. β-Actin was used as loading control. Densitometric quantification was shown in right. (G) The neonatal rat primary cardiomyocytes were challenged by HG at 33mM for indicated time and then MyD88/GAPDH was examined using Western blot assay. (H) The neonatal rat primary cardiomyocytes were challenged by HG at 33mM for indicated time and then MyD88 interaction with TLR2 or TLR4 was examined using Co-IP assay. Densitometric quantification was shown in right. Data were mean ± SEM. Scale bar=20 μm; n = 5 per group in panel A-E; n = 3 independent experiments in panel F-H; *P<0.05, **P<0.01 vs ctrl group.

Figure 2

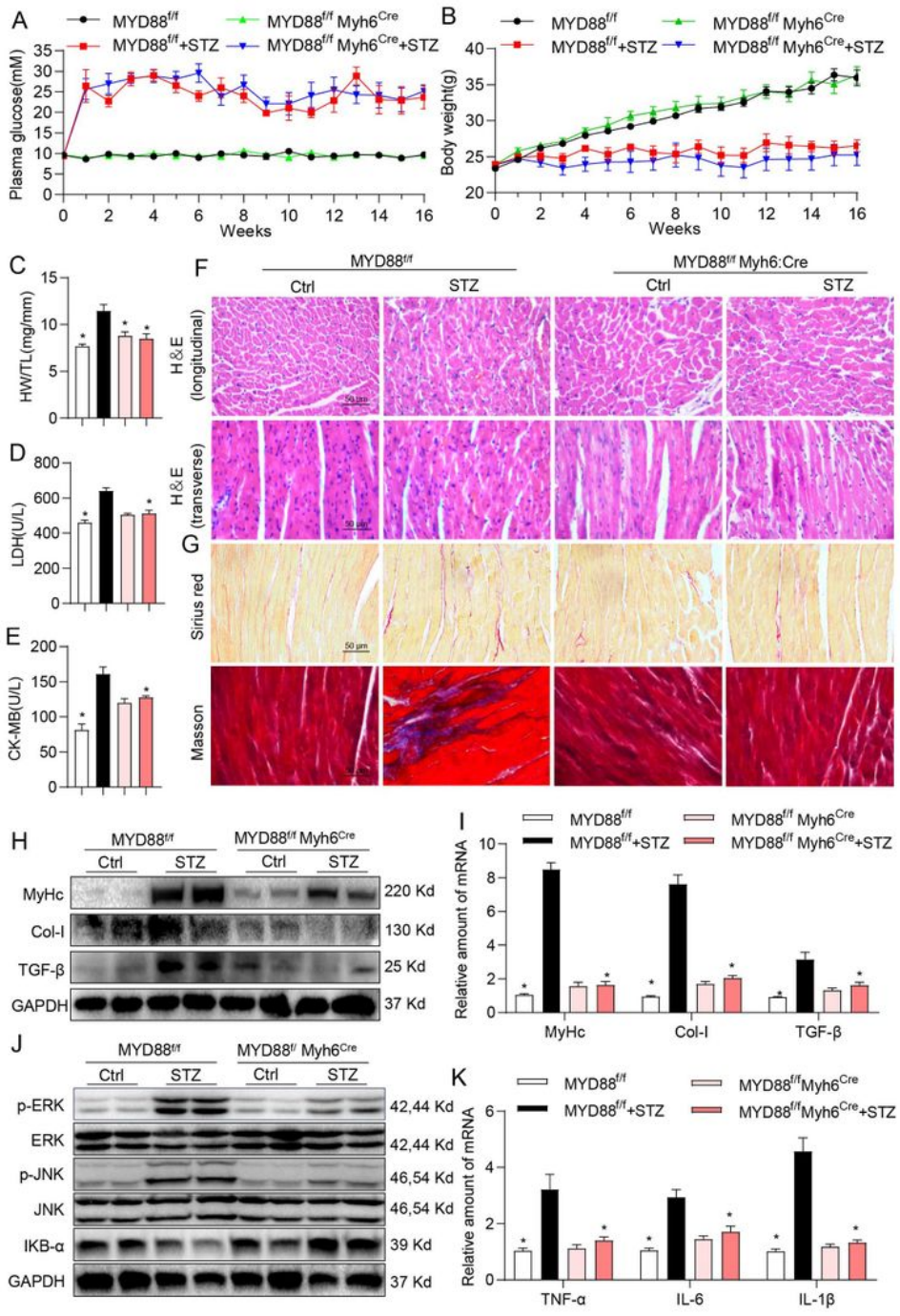

Figure 2

Cardiomyocyte-specific MyD88 knockout prevents STZ-induced cardiac inflammation and injury. Male MyD88f/f and MyD88f/f-Myh6Cre mice were injected with STZ (i.p. 50 mg/kg/day for 5 days) to induce T1DM. Fasting blood glucose (A) and body weight (B) were recorded weekly for 16 weeks. Heart tissue and blood samples were collected at termination for the determination of (C) heart weight/tibia length (HW/TL) ratios, (D) serum LDH and (E) serum CK-MB activity. Representative images (400X

magnification) of (F) H&E staining (longitudinal and transverse), (G) Sirius red and Masson's Trichrome staining of the heart tissues were shown. Representative western blot (H) and qPCR analysis (I) of MyHc, Col-I and TGF-β in the heart tissue were shown. (J) Levels of p-ERK, total ERK, p-JNK, total JNK, and IKB-α were determined by western blot. GAPDH was loading control. (K) qPCR analyses of TNF-α, IL-6 and IL-1β in the heart tissues were shown. Scale bar = 50 μm; n = 7 per group, *P<0.05 vs STZ-treated MYD88f/f group.

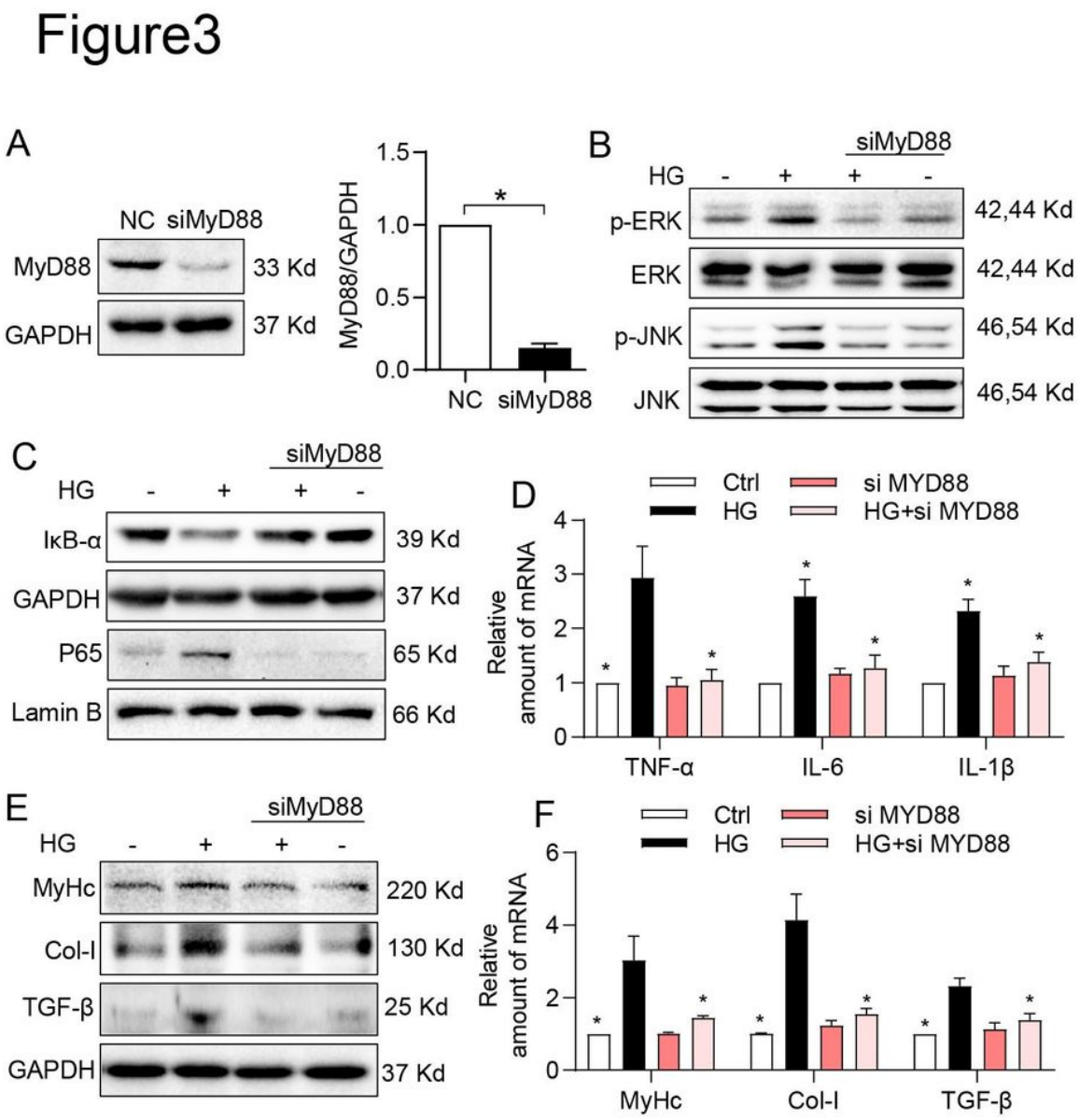

Figure 3

MyD88 knockdown attenuated high glucose-induced inflammation and fibrosis in cultured cardiomyocytes. H9c2 cells were transfected with either si-MyD88 or scrambled control siRNA (negative control) for 24 hours, and then treated with or without high glucose (HG; 33 mM). (A) MyD88 knockdown was confirmed by western blot. (B) Cells were treated with or without HG for 15 min. Protein levels of p-ERK, ERK, p-JNK and JNK were detected by western blot. (C) Cells were treated with or without HG for 15 min. IκB-α and nuclear p65 levels were detected by western blot. GAPDH and lamin B were corresponding loading controls. (D) Cells were treated with or without HG for 12 hours. Gene expression levels of TNF-α, IL-6 and IL-1β were detected by qPCR assay. (E) Cells were treated with or without HG for 24 hours. The protein levels of MyHc, Col-I and TGF-β were examined by Western blot assay. GAPDH was loading control. Densitometric quantification was shown in right. n = 3 independent experiments, *P<0.05 vs HG-treated cells.

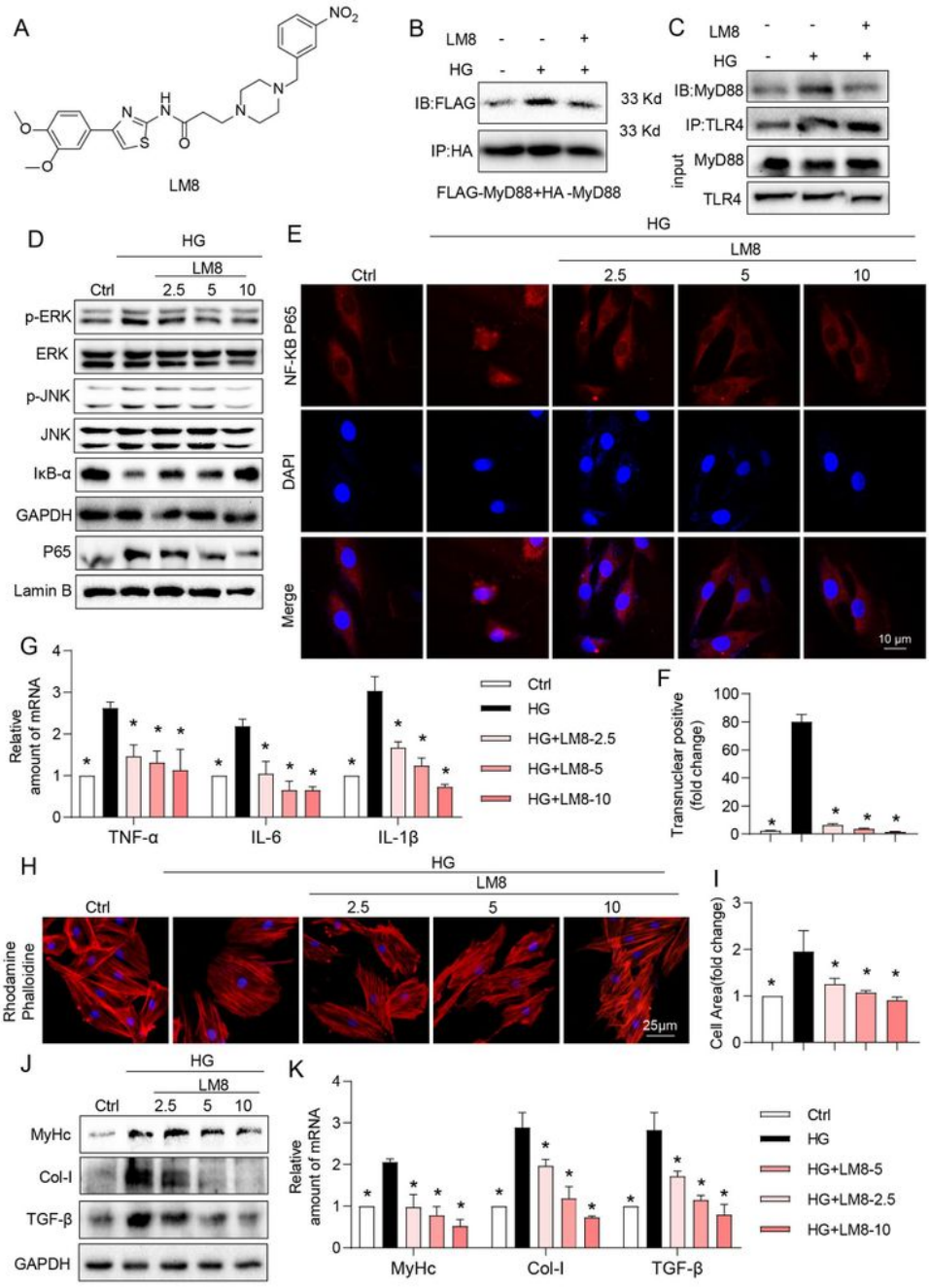

Figure 4

Pharmacological inhibition of MyD88 by LM8 protected cardiomyocytes against HG-induced inflammation and injuries. (A) Chemical structure of the MyD88 inhibitor LM8. (B) 293T cells were co-transfected with plasmids expressing Flag-MyD88 and HA-MyD88 for 24-hours, and then exposed to 33 mM glucose (HG) with or without LM8 for 15 min. MyD88 homodimers were detected by co-immunoprecipitation analysis. (C) Primary neonatal rat cardiomyocytes were pretreated with LM8 (10

μM) for 30 minutes before exposure to HG for 15 min. MyD88-TLR4 complexes were detected by co-IP analysis. (D) H9c2 cells were pretreated with LM8 at 2.5, 5 and 10 μM for 60-minutes, and then exposed to HG for 15 minutes. Protein levels of p-ERK, ERK, p-JNK, JNK and IκB-α and nuclear P65 were detected by western blot. (E, F) Representative images (scale bar = 10 μm) and quantitative analysis of P65 nuclear translocation were analysed by immunofluorescence staining in H9c2 cells pretreated with LM8 (2.5, 5 and 10 μM) and exposed to HG for 60 minutes. (G) H9c2 cells were pretreated with LM8 (2.5, 5 and 10 μM) for 60-minutes and then exposed to HG for 12 hours. Gene expression levels of TNF-α, IL-6 and IL1-β were determined by qPCR. (H, I) H9c2 cells were pretreated with 2.5, 5 or 10 μM MyD88 inhibitor LM8 and then exposed to HG for 24 hours. Representative image (scale bar = 25 μm) and bar graph show phalloidine-DyLight™ 554 stainings and quantification, respectively. H9c2 cells were pretreated with LM8 (2.5, 5 and 10 μM) and then exposed to HG for 24 h (for protein analysis) and 12 h (for qPCR analysis), respectively. (J-K) Protein levels (J) and gene expression levels (K) of MyHc, Col-I and TGF-β were determined by western blot and qPCR assay. n = 3 independent experiments, *P<0.05 vs HG-treated cells.

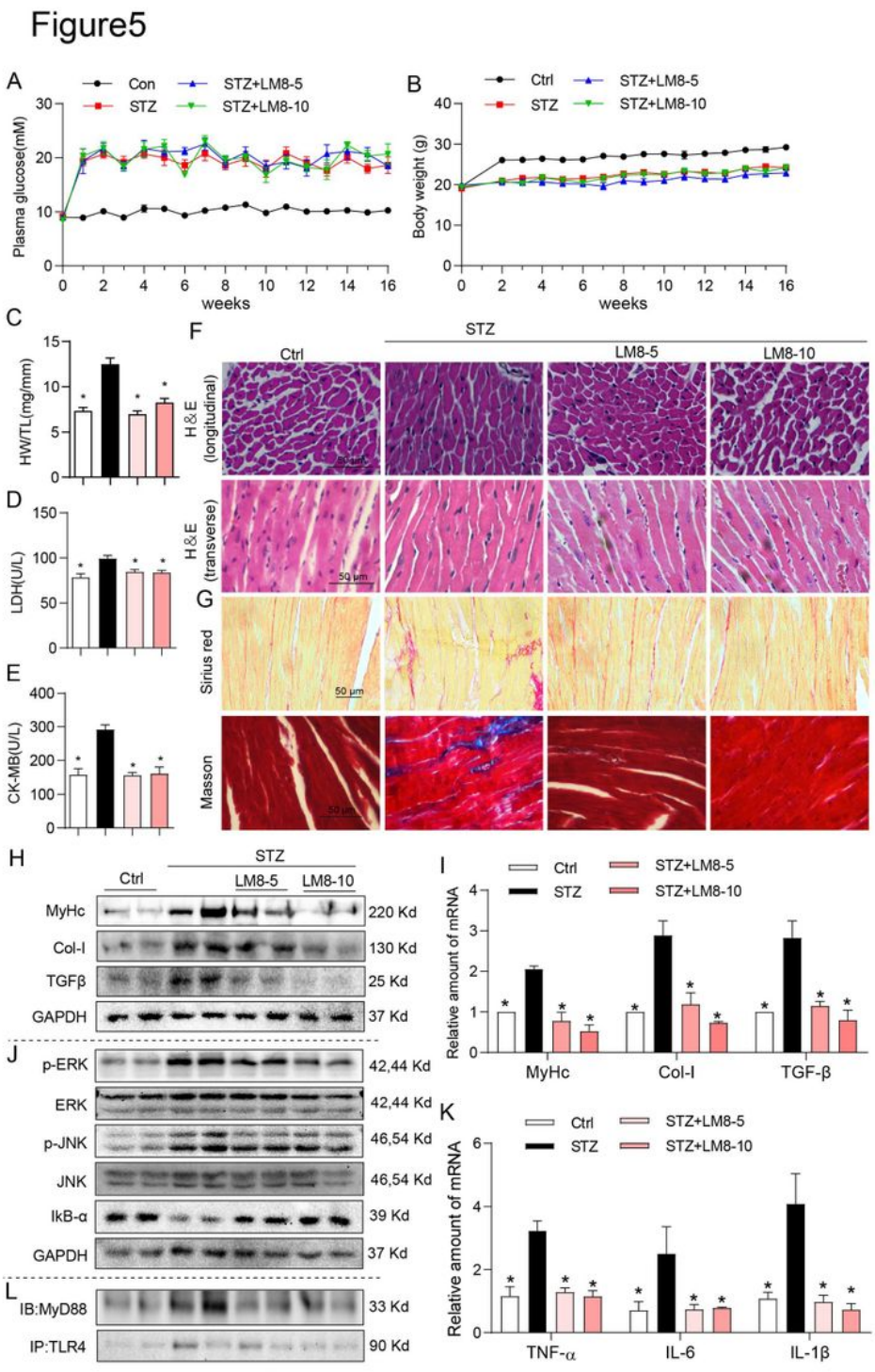

Figure 5

LM8 treatment prevented cardiac inflammation and injury in T1D mice. STZ-induced T1D mice were treated with vehicle or LM8 at 5 mg/kg (STZ+LM8-5) or 10 mg/kg (STZ+LM8-10) every other day. Fasting blood glucose (A) and body weight (B) were recorded weekly. Heart tissue and blood samples were collected at termination for the determination of (C) HW/TL ratios, (D) serum LDH and (E) serum CK-MB activity. Representative images (400X magnification, scale bar=50 μm) of (F) H&E staining (longitudinal

and transverse), (G) Sirius red and Masson's Trichrome staining of the heart tissues were shown. Representative western blot (H) and qPCR analysis (I) of MyHc, Col-I and TGF-β in the heart tissue were shown. (J) Levels of p-ERK, total ERK, p-JNK, total JNK, and IKB-α were determined by western blot. GAPDH was loading control. (K) qPCR analyses of TNF-α, IL-6 and IL-1β in the heart tissues were shown. (L) Co-IP analysis determined the interaction between TLR4 and MyD88 in the hearts. n = 7 per group, *P<0.05 vs STZ-treated group.

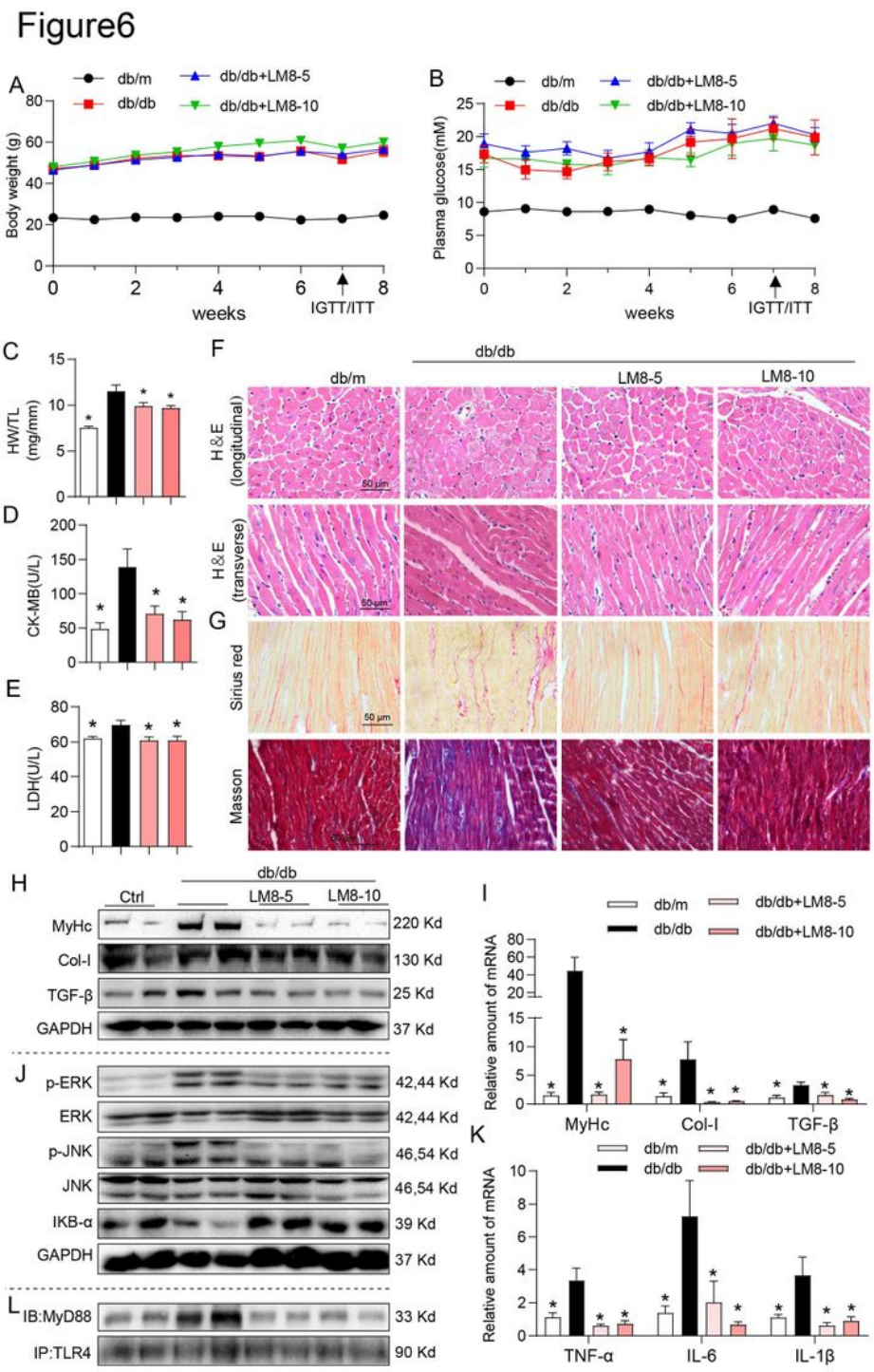

Figure 6

LM8 prevented cardiac inflammation and injury in db/db mice. Male db/db mice were treated with vehicle or LM8 at 5 (db/db+LM8-5) or 10 mg/kg (db/db+LM8-10) every other day for 8 weeks. The db/m mice treated with vehicle were controls. Fasting blood glucose (A) and body weight (B) were recorded weekly. Heart tissue and blood samples were collected at termination for the determination of (C) HW/TL ratios, (D) serum LDH and (E) serum CK-MB activity. Representative images (400X magnification, scale bar=50 μm) of (F) H&E staining (longitudinal and transverse), (G) Sirius red and Masson's Trichrome staining of the heart tissues were shown. Representative western blot (H) and qPCR analysis (I) of MyHc, Col-I and TGF-β in the heart tissue were shown. (J) Levels of p-ERK, total ERK, p-JNK, total JNK, and IKB-α were determined by western blot. GAPDH was loading control. (K) qPCR analyses of TNF-α, IL-6 and IL-1β in the heart tissues were shown. (L) Co-IP analysis determined the interaction between TLR4 and MyD88 in the hearts. n = 7 per group, *P<0.05 vs db/db group.

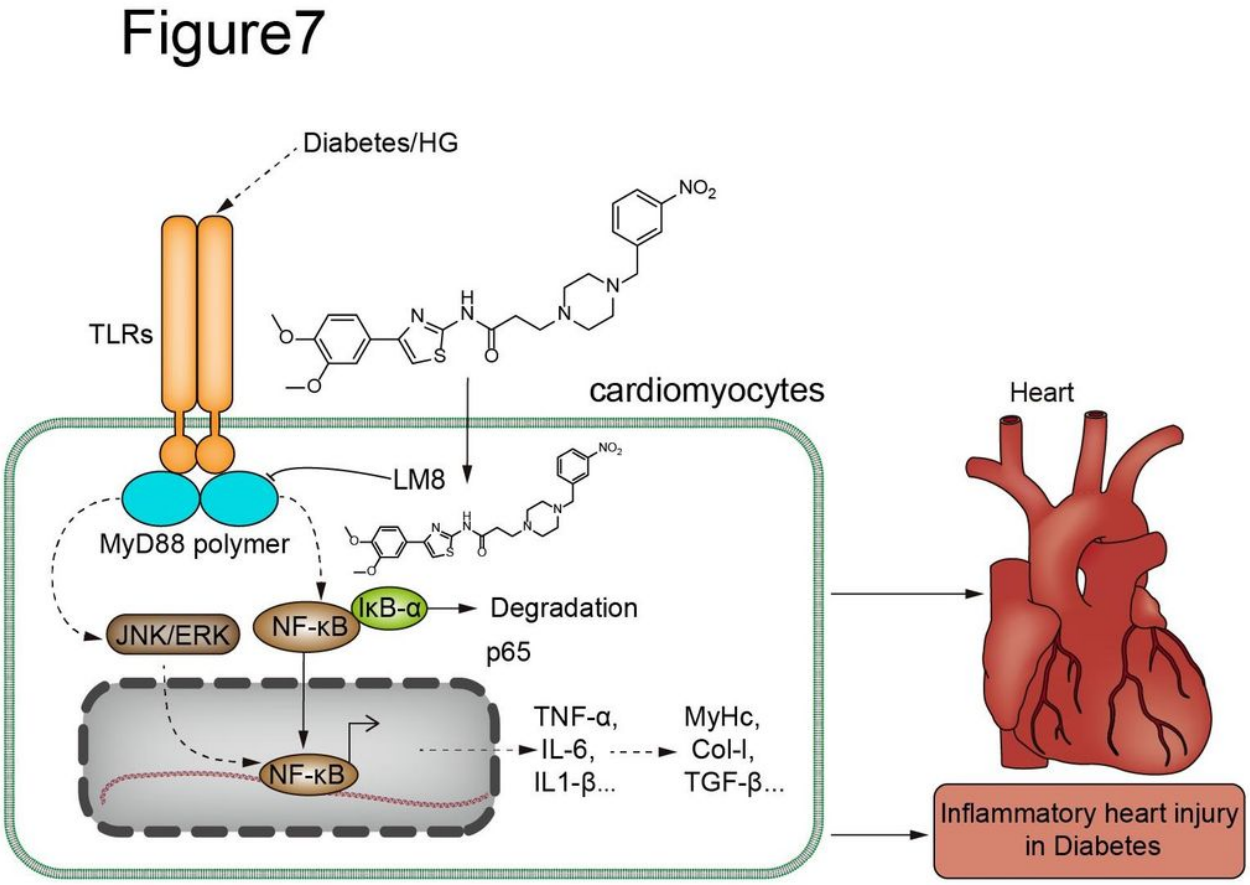

Figure 7

Schematic illustration of the underlying mechanism of MyD88 in diabetes/HG-induced inflammatory heart injuries.

Supplementary Files

This is a list of supplementary files associated with this preprint. Click to download.

- Supplementaryfile2021721.docx
- uncutedWBimage20210701.pdf